Electrical Transport and 1/f Noise in Semiconducting Carbon Nanotubes

Yu-Ming Lin,* Joerg Appenzeller, Zhihong Chen, and Phaedon Avouris

IBM T. J. Watson Research Center,

Yorktown Heights, NY 10598, USA

Abstract

We investigate electrical transport and noise in semiconducting carbon nanotubes. By studying carbon nanotube devices with various diameters and contact metals, we show that the ON-currents of CNFETs are governed by the heights of the Schottky barriers at the metal/nanotube interfaces. The current fluctuations are dominated by 1/f noise at low-frequencies and correlate with the number of transport carriers in the device regardless of contact metal.

Keywords: carbon nanotube, noise, Schottky barrier, FET

INTRODUCTION

Carbon nanotubes have attracted widespread attention as a unique low-dimensional electronic material since their discovery in the early 1990s [1, 2]. They are also actively explored for high performance nanoelectronics [3–5] owing to their exceptional electronic properties including quasi-ballistic transport and a current-carrying capability [6, 7]. One important application involves the use of semiconducting carbon nanotubes as the channel material of field-effect transistors [8, 9]. Over the last several years, much and rapid progress has been made to understand electrical properties and to explore the performance limit of carbon nanotube field-effect transistors (CNFETs). These nano-devices hold promises to sustain Moore's law in electronics even after the Si technology will reach its scaling limit. Integrated circuits based on carbon nanotubes, such as logic gates [10–12], and ring oscillators [13], have also been demonstrated.

The performance of a CNFET is critically dependent on the device geometry, nanotube diameter, and metal contacts. Conventional CNFETs usually operate as Schottky barrier-controlled devices [14, 15], referred as SB-CNFETs, where the current is modulated by the band profile at the metal/nanotube contact [16]. This SB-dominated transport results in large variation of ON-currents from device to device, a shallow switching slope [14], and undesirable scaling associated with the characteristic ambipolar behavior [17, 18]. To overcome some of the disadvantages, various device geometries and doping schemes have been developed for CNFETs [19–22] to enable a switching mechanism within the nanotube channel. Nevertheless, the Schottky barriers at the metal/nanotube contacts always play an essential role in governing the device ON-currents regardless of the switching mechanism.

In this paper, we report on recent experimental results of electrical current and its fluctuation behavior (i.e. noise) in CNFETs. In particular, we investigate the dependence of ON-currents of SB-CNFETs on the nanotube diameter and metal contact. These carbon nanotube devices exhibit pronounced 1/f-type current fluctuations at low frequencies. We find that while the device current is predominately determined by the Schottky barrier height [23], the 1/f fluctuations in carbon nanotubes are independent of metal contacts and only depend on the number of transport carriers in the device [24]. Possible means to reduce the noise in CNFETs are also discussed.

CONTACT-CONTROLLED ELECTRICAL TRANSPORT

Electrical properties of semiconducting carbon nanotubes are studied here using a standard back-gate configuration as shown in Fig. 1(a). In this setup, a carbon nanotube is used as the FET channel and is either dispersed from solution or directly grown on an oxidized silicon substrate, bridging the gap between the metal source and drain electrodes. The conducting Si substrate is used as the back gate electrode. Fig. 1(b) shows the typical subthreshold characteristics (drain current I_d as a function of gate voltage V_{gs}) of a back-gate carbon nanotube device with Ti metal contacts and a channel length of 600 nm. We note that the device is turned ON at both sufficiently negative and positive gate voltages, exhibiting ambipolar transistor characteristics. This ambipolar transport behavior results from the fact that the switching mechanism of a back-gate CNFET is dominated by the modulation of Schottky barriers (SBs) formed at the nanotube/metal contacts [14–16, 25]. The p- and n-branch of the CNFET characteristics are due to the tunneling of hole and electron carriers through the thinned SB at the source and drain contacts, respectively (see insets of Fig. 1(b)).

One of the key metrics that governs the transistor performance is the current of the device ON state I_{on}. Without loss of generality, we focus on the p-type branch of the SB-CNFET in the following discussion, and define I_{on} as the current at $V_{\mathrm{ds}} = V_{\mathrm{gs}} - V_{\mathrm{th}} = -0.5\,\mathrm{V}$. For SB-CNFETs, a wide range of ON-currents between 10^{-5} and 10^{-9} A have been reported by different groups for devices made from various nanotube sources (or diameters) and contact metals. This p-branch ON-current is dependent on the Schottky barrier height Φ_{SB-h} for hole carriers at the nanotube/metal interface, i.e. the line-up of the metal Fermi level and the valence band of the nanotube. In order to elucidate the impact of contact metal and the nanotube diameter on the device ON-currents, we have fabricated more than 100 SB-CNFETs with three different contact metals (Pd, Ti, and Al) and studied the statistics of their p-branch ON-currents. By comparing the diameter and I_{on} distribution of devices for each contact metal, the diameter dependence of I_{on} of Pd-, Ti-, Al-contacted CNFETs are summarized in Fig. 2 [23]. For any nanotube diameter, Pd-contacted CNFET delivers the highest I_{on} while Al-contacted devices have the lowest I_{on}. This is because Pd has the highest work function, which forms a small Φ_{SB-h} to the valence band of the nanotube. Since the nanotube band gap E_g is inversely proportional to the nanotube diameter, a

smaller Φ_{SB-h} is achieved for a larger diameter nanotube, leading to a monotonic increase of I_{on} with increasing nanotube diameter. One important trend observed in the semi-log plot of Fig. 2 is that I_{on} exhibits a stronger diameter dependence for small nanotubes than for large diameter nanotubes. The right axis of Fig. 2 shows the corresponding Schottky barrier height for hole carriers Φ_{SB-h}, which is extracted from I_{on} using an extended SB-CNFET transport model [23, 26].

In the SB-CNFET, the OFF-current, referred as the minimum current as a function of V_{gs}, is another important transistor property that defines the lower bound of the leakage current. As shown in Fig. 1(b), SB-CNFETs always possess an OFF-current that rises rapidly with increasing $|V_{\text{ds}}|$ due to the ambipolar characteristics [17]. Although OFF-currents of CNFETs usually increase exponentially with the nanotube diameter, the OFF-currents are much more susceptible to the environmental variations than the ON-currents, and care must be taken when attempting to experimentally acquire the dependence of I_{off} on the nanotube diameter and contact metal. As shown in Fig. 3, the OFF-current of a Ti-contacted CNFET varies by more than an order of magnitude after the device is covered with PMMA (Polymethyl-methacrylate) [27], while the ON-current remains almost unaffected. This is because, unlike the I_{on}, the OFF-current of the SB-CNFET is very sensitive to any uncontrolled charges adjacent to the nanotube (e.g. trap charges in the oxide) due to the small number of transport carriers in the device OFF state, making it challenging to obtain reliable and reproducible statistics of OFF-currents among different devices.

CURRENT FLUCTUATIONS IN CNFETS

While carbon nanotube FETs possess excellent DC electrical characteristics compared to the state-of-the-art Si MOSFETs, electrical measurements of these nano-devices usually appear to be noisier than most bulk materials. For nano-devices that involve only a small number of atoms or electrons, the noise signal due to statistical fluctuations can be quite significant and may impose additional optimization constraints for device performance and for applications. In view of the technological potential held by carbon nanotubes, it is necessary to understand the noise characteristics of these nano-devices.

Several types of electrical noises have been previously observed in carbon nanotubes, including the thermal noise associated with random Brownian motion, shot noise [28], random

telegraph signals [29], generation-recombination noises, and the 1/f-type fluctuations [30–32]. Here we focus on the so-called 1/f noise because it dominates the low-frequency fluctuations in a carbon nanotube device. As shown in Fig. 4, the current power spectrum S_I of a Pd-contacted SB-CNFET exhibits the distinct f^{-1} frequency dependence at various gate voltages. In the linear I_{d}-V_{ds} regime, S_I is proportional to I_{d}^2 (or V_{ds}^2) and can be expressed as $S_I = A_N \cdot I^2/f^{\beta}$, where A_N is defined as the 1/f noise amplitude and $\beta \simeq 1$. In Figs. 5(a) and (b), we plot the subthreshold characteristics and the measured noise amplitude A_N of the Pd-contacted CNFET, respectively, showing that the noise level A_N increases by more than three orders of magnitude as the CNFET is switched from the ON to the OFF state.

This gate-dependent $1/f$ noise in semiconducting nanotubes is found to be related to the total number of transport carriers N in the channel [24], described by an empirical relation

$$A_N = \frac{\alpha_H}{N}, \tag{1}$$

where N is the number of carriers in the system and α_H is a parameter that may vary from device to device. This $A \propto 1/N$ dependence was first introduced by Hooge [33] to describe the 1/f noise results in homogenous bulk materials. Although α_H is not a universal constant, $\alpha_H \sim 10^{-3}$ is a value frequently found in non-optimized bulk materials [34].

In order to extract the parameter α_H in a carbon nanotube device, we adopt the extended SB-CNFET model described in Ref. [26], which is based on the non-equilibrium Green's function formalism[35], to calculate the device current and the carrier number N as a function of gate voltage V_{gs}. Using $\alpha_H = 2 \times 10^{-3}$, the simulated current and noise amplitude N_A of the Pd-CNFET are shown as the solid curves in Fig. 5(a) and (b), respectively, both exhibiting excellent agreement with experimental data. It is important to note that this $1/f$ noise parameter $\alpha_H = 2 \times 10^{-3}$ determined for CNFETs that consist of unpurified carbon nanotube is quite comparable to the value observed in most bulk systems. The pronounced $1/f$ noise amplitude A_N observed in carbon nanotubes is therefore due to a much smaller N value in the device rather than a material-specific property. It should be noted that because of the finite transmission probability at the nanotube/metal contacts and the associated delocalized nature of the electron/hole wave functions, the calculated carrier number N is not necessarily an integer and can be smaller than unity near the OFF state. In addition to the gate-dependent studies presented here, this 1/N scaling behavior of 1/f noise has also been observed in the length-dependent experiments of CNFETs [24, 36].

In Fig. 5, we show the subthreshold characteristics and the 1/f noise amplitude of a Ti-contacted CNFET with the same device geometry. Compared to the Pd-CNFET, the Ti-CNFET delivers a lower ON-current as expected. Interestingly, the two CNFETs possess comparable A_N values in the ON state and exhibit similar gate dependence for A_N (see Fig. 5(b)). This is because in an SB-CNFET, the tunneling current is dependent on the SB height while the number N of holes inside the nanotube remains independent of Φ_{SB-h} for a given gate voltage (relative to the threshold voltage) [37]. The results also suggest that while the transport of an SB-CNFET is dominated by the tunneling through the Schottky barrier, the $1/f$ noise, however, is not entirely determined by the contacts.

To further examine the role of the SB contacts on the 1/f noise, we have fabricated dual-gate CNFETs [38], where a middle Al gate stack is placed underneath the nanotube between the source/drain electrodes (see Fig. 6(a)). In contrast to the SB-CNFET, the transistor operation of the dual-gate CNFET is achieved by the Al gate voltage that controls the potential barrier within the nanotube channel in a way similar to that of conventional MOSFETs [19]. With the dual-gate structure, the band-bending at the contacts and in the nanotube channel can be independently controlled, making it possible to distinguish their roles in the noise behavior. As shown in Fig. 6(b), at a given Si back-gate voltage, the noise amplitude A_N increases with the resistance as $V_{\mathrm{gs-Al}}$ varies. Since the SB potential profile in the dual-gate CNFET is unchanged at a constant $V_{\mathrm{gs-Si}}$, this significant variation of A_N as a function of $V_{\mathrm{gs-Al}}$ is due to the modulation of N by the potential barrier in the nanotube channel. The result also indicates that the 1/f noise in a CNFET is not entirely specified by properties of the SB at the metal/nanotube interface, consistent with the observation in Fig. 5(b) for different contact metals. We also observe that, for the same Al gate voltage, the dual-gate CNFET possesses a higher 1/f noise level at $\mathrm{V_{gs-Si}} = -1.5\,\mathrm{V}$ compared to that at $V_{\mathrm{gs-Si}} = -2.5\,\mathrm{V}$ (see Fig. 6(b)). This is because the number of carriers for a given $V_{\mathrm{gs-Al}}$ is smaller due to the lower transmission probability through the SB modulated by $V_{\mathrm{gs-Si}}$. The results here illustrate that the 1/f noise level in a semiconducting nanotube is not solely determined by either the contact or channel characteristics.

In carbon nanotube devices, the $A_N \propto 1/N$ dependence has been observed in both diffusive and quasi-ballistic transport regimes with comparable α_H values ($\sim 10^{-3}$) [24, 36] suggesting that the origin of 1/f noise in carbon nanotubes does not coincide with the scattering processes determining their dc electrical characteristics. In fact, while dc electrical

measurements show quasi-ballistic transport in carbon nanotubes for a channel length of 600 nm as used in our study, the conduction channel in the actual devices is far from an ideal one without perturbations with respect to noise considerations. In particular, since these CNFETs are fabricated on unpassivated oxide substrates, one important origin of the 1/f noise is the random trapping and detrapping of charges in the nanotube/oxide interface that modulates the number of carriers and the surface potential, as in Si MOSFETs. We note that despite the significance of trapping/detrapping process on the 1/f noise, the transport of the CNFETs remains quasi-ballistic as evident from by the almost perfect absence of a length dependent resistance. Thus, the observed 1/f noise in these CNFET devices is not due to intrinsic processes of carbon nanotube, but is rather associated with external fluctuation sources, which can ne quantitatively characterized by the factor α_H. Nevertheless, the noise amplitude A_N of the CNFET is related to one important intrinsic parameter of the nanotube – the number of carriers N – as described by Eq. (1).

It is expected that 1/f noise in carbon nanotube devices can be reduced by eliminating some of the external fluctuation sources, e.g. charge traps in the oxide, thus lowering α_H. In this respect, it has been recently shown that A_N in a carbon nanotube device can be effectively lowered by more than an order of magnitude through a proper annealing process [39]. In practical applications, it has been proposed to use an array of parallel nanotubes or multiple contacts on a single long nanotube in order to provide high drive currents [37]. This design, in principle, can also lead to a reduction of A_N by factor given through the nanotube multiplicity.

CONCLUSION

In this article, we have investigated electrical transport and noise behaviors in semiconducting nanotubes. The ON-currents of CNFETs are governed by the height of the Schottky barriers at the metal/nanotube interface, which is a function of the nanotube diameter and contact metal. By studying more than a hundred CNFET devices, we have established the quantitative correlation between the p-type ON-currents and the nanotube diameter for various metal contact, showing that larger diameter nanotubes are favorable for delivering higher ON-currents. The current fluctuation in CNFETs is dominated by the 1/f noise at low frequencies. Despite the important role of SB for the ON-current of the injection-

controlled devices, we find that the noise amplitude of CNFETs is inversely proportional to the number of transport carriers in the device regardless of contact metal.

* Electronic address: `yming@us.ibm.com`

[1] S. Iijima and T. Ichihashi, Nature(London) **363**, 603 (1993).

[2] D. S. Bethune, C. H. Kiang, M. S. Devries, G. Gorman, R. Savoy, J. Vazquez, and R. Beyers, Nature **363**, 605 (1993).

[3] Ph. Avouris, J. Appenzeller, R. Martel, and S. J. Wind, Proc. of the IEEE **91**, 1772 (2003).

[4] P. L. McEuen, M. S. Fuhrer, and H. Park, IEEE Trans. Nanotechnology **1**, 78 (2002).

[5] J. Appenzeller, R. Martel, V. Derycke, M. Radosavljevic, S. J. Wind, D. Neumayer, and Ph. Avouris, Microelectronic Engineering **64**, 391 (2002).

[6] Z. Yao, C. L. Kane, and C. Dekker, Phys. Rev. Lett. **84**, 2941 (2000).

[7] A. Javey, J. Guo, D. B. Farmer, Q. Wang, E. Yenilmez, R. G. Gordon, M. Lundstrom, and H. Dai, Nano Lett. **4**, 1319 (2004).

[8] R. Martel, T. Schmidt, H. R. Shea, T. Hertel, and Ph. Avouris, Appl. Phys. Lett. **73**, 2447 (1998).

[9] S. T. Tans, A. R. M. Verschueren, and C. Dekker, Nature **393**, 49 (1998).

[10] V. Derycke, R. Martel, J. Appenzeller, and Ph. Avouris, Nano Lett. **1**, 453 (2001).

[11] A. Bachtold, Ph. Hadley, T. Nakanishi, and C. Dekker, Science **294**, 1317 (2001).

[12] A. Javey, Q. Wang, A. Ural, Y. Li, and H. Dai, Nano Lett. **2**, 929 (2002).

[13] Z. Chen, J. Appenzeller, Y.-M. Lin, J. Sippel-Oakley, A. G. Rinzler, J. Tang, S. J. Wind, P. M. Solomon, and Ph. Avouris, Science **311**, 1735 (2006).

[14] J. Appenzeller, J. Knoch, V. Derycke, R. Martel, S. Wind, and Ph. Avouris, Phys. Rev. Lett. **89**, 126801 (2002).

[15] S. Heinze, J. Tersoff, R. Martel, V. Derycke, J. Appenzeller, and Ph. Avouris, Phys. Rev. Lett. **89**, 106801 (2002).

[16] M. Freitag, M. Radosavljevic, Y. X. Zhou, A. T. Johnson, and W. F. Smith, Appl. Phys. Lett. **79**, 3326 (2001).

[17] M. Radosavljevic, S. Heinze, J. Tersoff, and Ph. Avouris, Appl. Phys. Lett. **83**, 2435 (2003).

[18] S. Heinze, M. Radosavljevic, J. Tersoff, and Ph. Avouris, Phys. Rev. B **68**, 235418 (2003).

[19] Y.-M. Lin, J. Appenzeller, J. Knoch, and Ph. Avouris, IEEE Trans. Nanotechnology **4**, 481 (2005).

[20] J. Chen, C. Klinke, A. Afzali-Ardakani, and Ph. Avouris, Appl. Phys. Lett. **86**, 123108 (2005).

[21] A. Javey, J. Guo, D. B. Farmer, Q. Wang, D. Wang, R. G. Gordon, M. Lundstrom, and H. Dai, Nano Lett. **4**, 447 (2004).

[22] J. Appenzeller, Y.-M. Lin, J. Knoch, Z. Chen, and Ph. Avouris, IEEE Trans. Electron Device pp. 2568–2576 (2005).

[23] Z. Chen, J. Appenzeller, J. Knoch, Y.-M. Lin, and Ph. Avouris, Nano. Lett. **5**, 1497 (2005).

[24] Y.-M. Lin, J. Appenzeller, J. Knoch, Z. Chen, and Ph. Avouris, Nano Lett. **6**, 930 (2006).

[25] R. Martel, V. Derycke, C. Lavoie, J. Appenzeller, K. K. Chan, J. Tersoff, and Ph. Avouris, Phys. Rev. Lett. **87**, 256805 (2001).

[26] J. Knoch and J. Appenzeller, in *Hardware Technology Drivers of Ambient Intelligence*, Chap. 6.2 (Kluwer: Dordrecht, 2006).

[27] A. Javey, Q. Wang, W. Kim, and H. Dai, IEDM technol. Dig. p. 741 (2003).

[28] P.-E. Roche, M. Kociak, S. Gueron, A. Kasumov, B. Reulet, and H. Bouchiat, Eur. Phys. J. B **28**, 217 (2002).

[29] F. Liu, M. Bao, H.-J. Kim, K. L. Wang, C. Li, X. Liu, and C. Zhou, Appl. Phys. Lett. **86**, 163102 (2005).

[30] P. G. Collins, M. S. Fuhrer, and A. Zettl, Appl. Phys. Lett. **76**, 894 (2000).

[31] H. W. C. Postma, T. F. Teepen, Z. Yao, and C. Dekker, in *Proceedings of XXXVI th Rencontre De Moriond* (EDP Sciences, France, 2001).

[32] E. S. Snow, J. P. Novak, M. D. Lay, and F. K. Perkins, Appl. Phys. Lett. **85**, 4172 (2004).

[33] F. N. Hooge, Phys. Lett. **29A**, 139 (1969).

[34] F. N. Hooge, IEEE Trans. Electron Devices **41**, 1926 (1994).

[35] S. Datta, Superlatt. Microstructure **28**, 253 (2000).

[36] M. Ishigami, J. Chen, E. Williams, D. Tobias, Y. Chen, and M. Fuhrer, Appl. Phys. Lett. **88**, 203116 (2006).

[37] J. Appenzeller, Y.-M. Lin, J. Knoch, Z. Chen, and Ph. Avouris, submitted.

[38] Y.-M. Lin, J. Appenzeller, Z. Chen, Z.-G. Chen, H.-M. Chen, and Ph. Avouris, IEEE Electron Device Lett. **26**, 823 (2005).

[39] Y.-M. Lin, J. Appenzeller, C. C. Tsuei, Z. Chen, and Ph. Avouris, in *64th Device Research Conference Digest* (IEEE, 2006), p. 279.

Figure Caption

Figure 1: (a) Schematics of a back-gate carbon nanotube field-effect transistor. A highly-doped Si substrate is usually used as the back gate. (b) Measured subthreshold characteristics of a Ti-contacted CNFET on 10-nm SiO_2. The source-drain separation is 600 nm, and the nanotube diameter is about 1.8 nm. The source electrode is grounded and the drain voltages are -0.1, -0.5 and -0.9 V. The insets illustrate the schematic band diagrams at negative and positive gate voltages, where the tunneling of hole and electron carriers is enabled at the source and drain electrodes, respectively.

Figure 2: Measured I_{on} of CNFETs as a function of nanotube diameter for Pd, Ti, and Al metal contacts [23]. The CNFETs are fabricated on 10-nm SiO_2, and I_{on} is measured at $V_{\mathrm{ds}} = V_{\mathrm{gs}} - V_{\mathrm{th}} = -0.5\,\mathrm{V}$ for all devices. The right axis is the Schottky barrier height for hole carriers Φ_{SB-h} extracted from I_{on} using the extended SB-CNFET model calculation.

Figure 3: Comparison of the subthreshold characteristics of a Ti-contacted CNFET before and after the device is covered with PMMA. The OFF-current is lowered by more than an order of magnitude after the PMMA passivation, whereas the ON-current remains unaffected.

Figure 4: Normalized current noise power spectrum (S_I/I^2) of a Pd-contacted CNFET at various gate voltages. The drain bias is kept at 10 mV. The solid line indicates the 1/f dependence of the noise power spectrum.

Figure 5: (a) Subthreshold characteristics of CNFETs with Pd and Ti metal contacts. The drain voltage is 10 mV. Both devices are fabricated on 10-nm SiO_2 with a channel length of 600 nm. The solid curve is the simulated current for the Pd-CNFET. (b) Measured noise amplitude A_N as a function of gate voltage for the two CNFETs shown in (a). The solid curve is the simulated noise amplitude of the Pd-CNFET based on Eq. (1). The extracted α_H value is 2×10^{-3}

Figure 6:(a) Schematics of a dual-gate CNFET, where an additional middle gate stack,

normally a metal electrode covered with a layer of oxide, is placed underneath the nanotube between the source and drain electrode. In our study, the middle gate stack consists of Al_2O_3/Al with a width of 40 nm. The source and drain electrodes are made of Pd. (b) The drain current (left axis) and 1/f noise amplitude A (right axis) of the dual-gate CNFET as a function of Al gate voltage $V_{\mathrm{gs-Al}}$ of the dual-gate CNFET for two Si backgate voltages $V_{\mathrm{gs-Si}}$ =-2.5 V and -1.5 V [24]. The drain voltage is 10 mV.

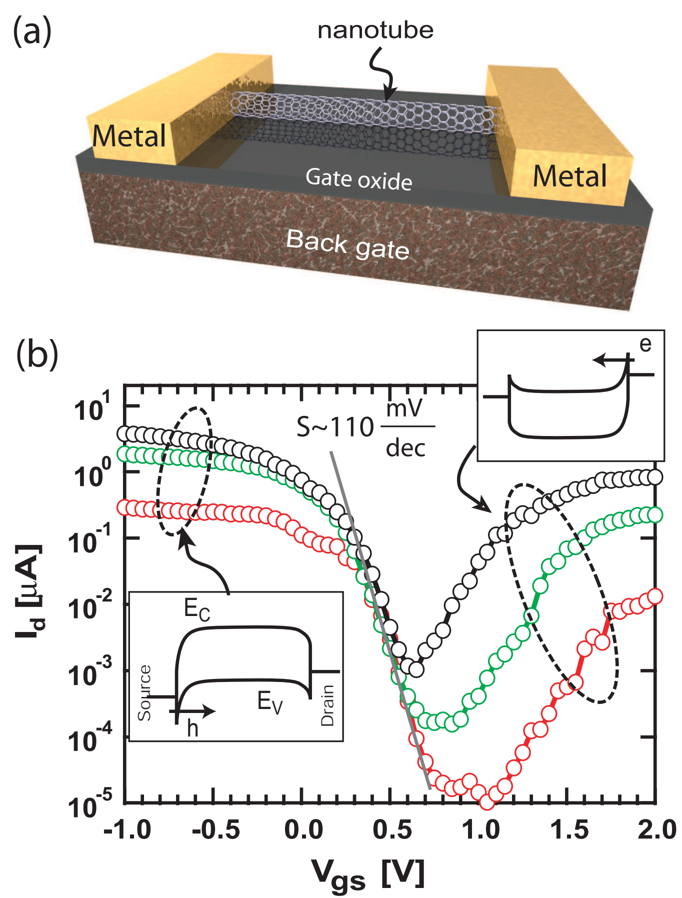

FIG. 1: Lin et al.

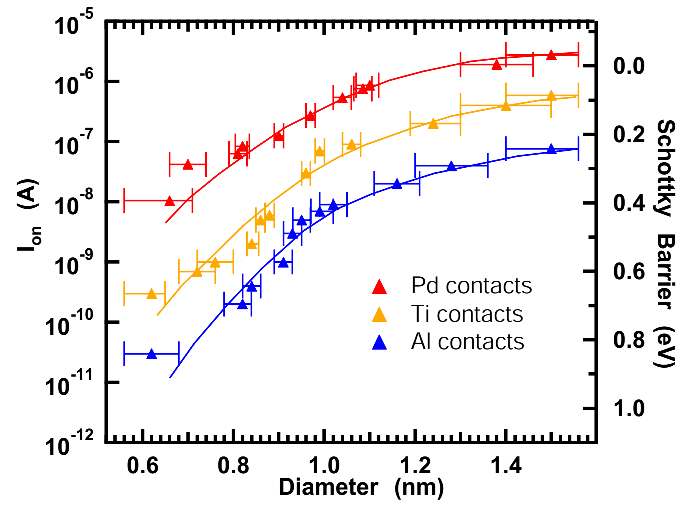

FIG. 2: Lin et al.

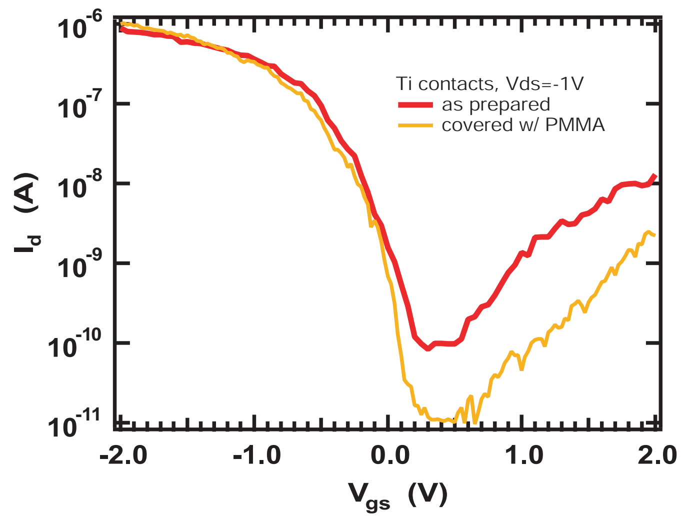

FIG. 3: Lin et al.

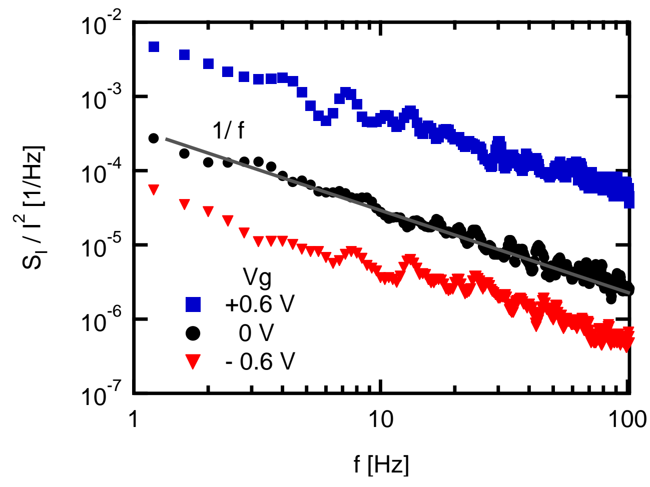

FIG. 4: Lin et al.

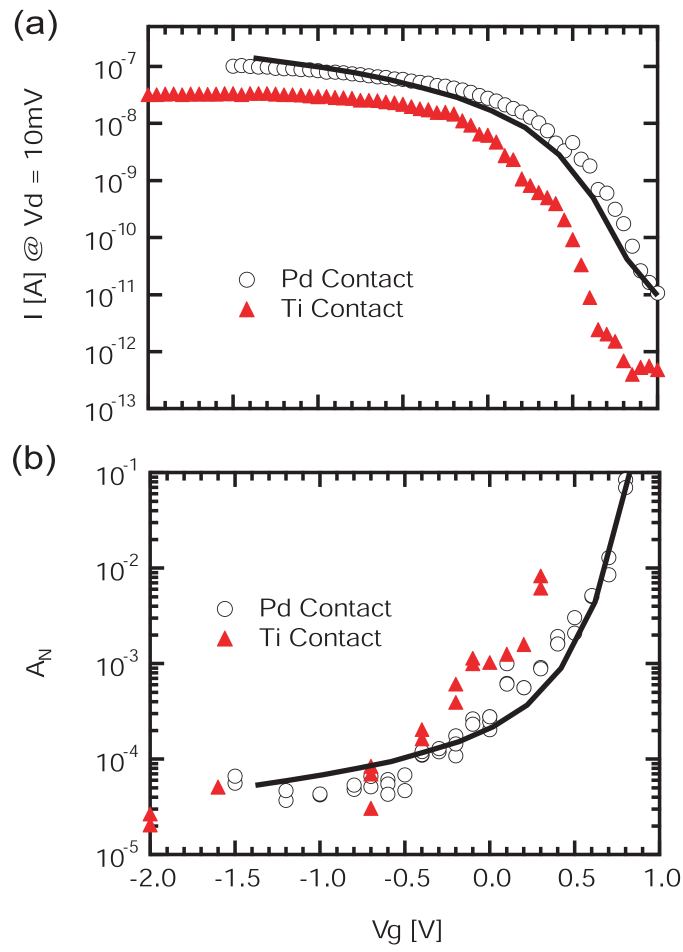

FIG. 5: Lin et al.

(a)

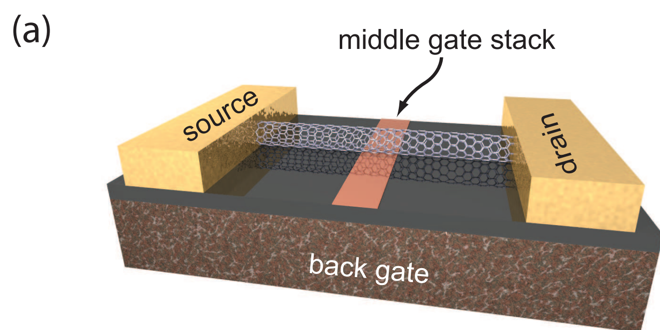

(b)

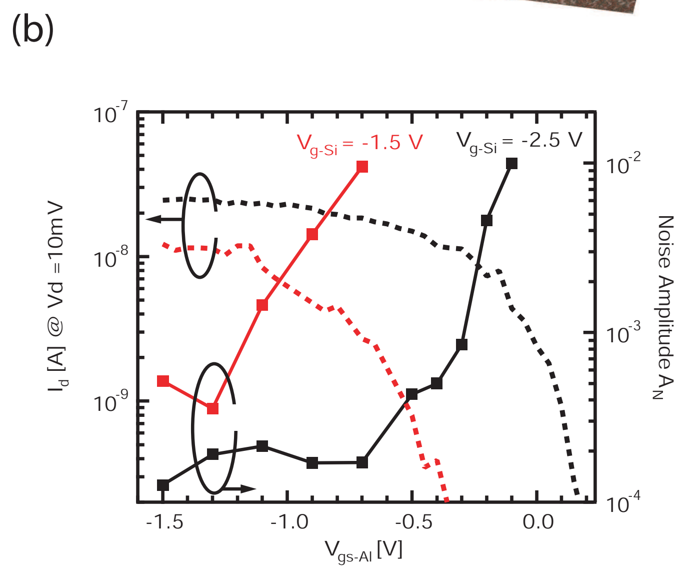

FIG. 6: Lin et al.